

Facial-Meridional Isomerization of Some Tris-(β -diketonato)ruthenium(III) Complexes

Kyohko KOBAYASHI, Yuichi SATSU, Yoshimasa HOSHINO, Shinji ARAI, Kiyoshi HATAKEYAMA, Akira ENDO, Kunio SHIMIZU, and Gen P. SATÔ*

Department of Chemistry, Faculty of Science and Technology,
Sophia University, 7-1 Kioicho, Chiyoda-ku, Tokyo 102

(Received May 31, 1989)

Nine complexes of type $[\text{Ru}^{\text{III}}(\text{R}-\text{CO}-\text{CH}-\text{CO}-\text{R}')_3]$ were examined; only those with $\text{R}=\text{CF}_3$ underwent the facial-meridional isomerization in *N,N*-dimethylformamide (DMF) at the reflux temperature. Qualitative examination of the occurrence of isomerization of the complex with $\text{R}=\text{CF}_3$ and $\text{R}'=\text{CH}_3$ in various solvents supports the presence of solvent-assisted bond-rupture mechanisms. This complex did not isomerize photochemically in acetonitrile. The isomerization of four complexes with $\text{R}=\text{CF}_3$ and $\text{R}'=\text{CH}_3$, $-\text{C}_2\text{H}_5$, $-\text{CH}(\text{CH}_3)_2$, and $-\text{C}(\text{CH}_3)_3$ in DMF at 70–100 °C followed the reversible first-order kinetics. The equilibrium constants, which were temperature independent, decreased from 4.27 to 1.74 in the order cited above. The enthalpies of activation, ranging from 66.4 kJ mol⁻¹ ($\text{R}'=\text{CH}(\text{CH}_3)_2$) to 96.0 kJ mol⁻¹ ($\text{R}'=\text{CH}_3$), depended linearly on the atomic bond populations of the Ru–O bonds calculated by means of a modified extended Hückel method.

The facial-meridional isomerization reactions of tris(unsymmetrical β -diketonato)metal chelates have been studied in a number of cases.^{1–8)} Tris(β -diketonato)ruthenium(III) complexes are known to behave as “slow” complexes in the isomerization and racemization reactions.^{4,5)} These reactions are believed to proceed through intramolecular, bond-rupture mechanisms. Recently Hoshino et al.⁹⁾ reported that the rearrangement reactions between the three geometrical isomers of acetylacetonatobis(4,4,4-trifluoro-1-phenyl-1,3-butanedionato)ruthenium(III) proceeded through certain types of bond-rupture mechanisms.

The rate of the facial-meridional isomerization reaction is largely enhanced by the presence of a trifluoromethyl group at the β -position of the diketone.⁴⁾ It is of interest to see how the substituents of the β -diketonato ligands affect the rate of the isomerization.

This report presents qualitative observations on the facial-meridional isomerization reactions of a series of nine tris(substituted acetylacetonato)ruthenium(III)

complexes and quantitative kinetic data for four of them.

Experimental

Preparation of Complexes. The complexes studied here are listed in Table 1 together with the ligand names. They will be cited by the numbers given there. The preparation of **1**, **4**, and **6–9** has been described previously.¹⁰⁾ Each of them, except **6** and **7**, was obtained as a mixture of geometri-

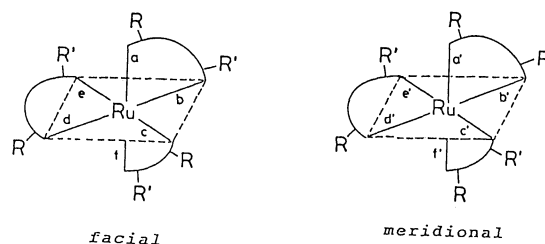


Fig. 1. Geometrical isomers of a tris(unsymmetrical β -diketonato)ruthenium complex and their bond designations.

Table 1. Numbers of the Complexes $[\text{Ru}^{\text{III}}(\text{R}-\text{CO}-\text{CH}-\text{CO}-\text{R}')_3]$, Their Reactions, and the Ligand Names

No.	R	R'	Reaction in DMF ^{a)}	Ligand name
1	$-\text{CF}_3$	$-\text{CH}_3$	i	1,1,1-Trifluoro-2,4-pentanedionato
2^{b)}	$-\text{CF}_3$	$-\text{C}_2\text{H}_5$	i	1,1,1-Trifluoro-2,4-hexanedionato
3^{b)}	$-\text{CF}_3$	$-\text{CH}(\text{CH}_3)_2$	i	1,1,1-Trifluoro-5-methyl-2,4-hexanedionato
4	$-\text{CF}_3$	$-\text{C}(\text{CH}_3)_3$	i	1,1,1-Trifluoro-5,5-dimethyl-2,4-hexanedionato
5^{b)}	$-\text{C}_2\text{H}_5$	$-\text{CH}_3$	n	2,4-Hexanedionato
6^{c)}	$-\text{CH}_3$	$-\text{C}(\text{CH}_3)_3$	n	5,5-Dimethyl-2,4-hexanedionato
7^{c)}	$-\text{CF}_3$	$-\text{C}_4\text{H}_9\text{S}$	r	4,4,4-Trifluoro-1-(2-thienyl)-1,3-butanedionato
8	$-\text{CF}_3$	$-\text{C}_4\text{H}_9\text{O}$	r	4,4,4-Trifluoro-1-(2-furyl)-1,3-butanedionato
9	$-\text{CF}_3$	$-\text{C}_6\text{H}_5$	r	4,4,4-Trifluoro-1-phenyl-1,3-butanedionato

a) Reaction observed when the complex was refluxed in DMF: i, isomerization; n, no isomerization; r, reduction to the Ru^{II} species. b) New compound. c) Only the meridional form was obtained.

cal isomers: the facial and the meridional forms (Fig. 1). The samples of **6** and **7**, however, contained only the meridional forms. The isomeric mixtures of **2**, **3**, and **5** were prepared by means of the "ruthenium blue solution" method.¹⁰ 1,1,1-Trifluoro-2,4-hexanedione and 1,1,1-trifluoro-5-methyl-2,4-hexanedione were prepared according to the method of Reid and Calvin,¹¹ while 2,4-hexanedione was purchased from Dojindo Laboratories.

Isolation of Isomers. The isomeric mixture of **1**, dissolved in a small volume of benzene, was applied to a column of Merck Kieselgel 60 and developed with a benzene-hexane mixture (volume ratio, 5:8). Fractions containing each of the pure isomers were combined, and the solvent was evaporated off. The residue was dissolved in ethanol. Crystals of each isomer were obtained on concentrating the ethanolic solution. The fractions containing incompletely separated isomers were collected and concentrated; the isomers therein were then separated by means of preparative thin-layer chromatography on Merck Kieselgel 60 plate (1 mm thick, 20×20 cm), developing agent being a benzene-hexane mixture (volume ratio, 1:1). Separation of the isomers of **2**, **3**, **4**, and **8** was carried out similarly on the silica-gel column with benzene-hexane mixtures (the volume ratios were 1:9 for **2** and **3**, 1:4 for **4**, and 1:1 for **8**). The meridional isomer preceded the facial isomer in every case. In the case of **5**, only partial separation was achieved by means of Kieselgel 60—chloroform preparative thin-layer chromatography: the meridional form was completely separated from the facial isomer, but the latter could not be obtained in pure state. Separation of the isomers of **9** has been described previously.¹² No attempt was made at resolving the optical isomers.

Complexes **2**, **3**, and **5** are new compounds. Their elemental analyses and ¹H NMR data are as follows: **2** Found: C, 35.73 (*fac*) and 35.79 (*mer*); H, 2.89 (*fac*) and 2.97% (*mer*). Calcd for RuC₁₈H₁₈O₆F₉: C, 35.89; H, 3.01%. **3** Found: C, 39.05 (*fac*) and 38.94 (*mer*); H, 3.70 (*fac*) and 3.65% (*mer*). Calcd for RuC₂₁H₂₄O₆F₉: C, 39.14; H, 3.75%. **5** Found (isomeric mixture): C, 48.82; H, 6.21%. Calcd for RuC₁₈H₂₇O₆: C, 49.08; H, 6.18%. ¹H NMR (CDCl₃, room temp): *fac*-**2** δ =−36.1 (3H, s, CH), −4.8 (3H, s, CH₂), −4.3 (3H, s, CH₂), 3.0 (9H, s, CH₃); *mer*-**2** δ =−52.9 (1H, s, CH), −42.9 (1H, s, CH), −26.2 (1H, s, CH), −13.5 (1H, s, CH₂), −12.2 (1H, s, CH₂), −7.7 (1H, s, CH₂), −7.0 (1H, s, CH₂), −2.5 (1H, s, CH₂), −2.0 (1H, s, CH₂), 1.6 (3H, s, CH₃), 1.8 (3H, s, CH₃), 3.2 (3H, s, CH₃); *fac*-**3** δ =−36.4 (3H, s, COCHCO), −2.7 (3H, s, (CH₃)₂CH), 2.3 (9H, s, CH₃), 3.7 (9H, s, CH₃); *mer*-**3** δ =−51.2 (1H, s, COCHCO), −41.0 (1H, s, COCHCO), −28.4 (1H, s, COCHCO), −7.9 (1H, s, (CH₃)₂CH), −4.6 (1H, s, (CH₃)₂CH), −1.8 (1H, s, (CH₃)₂CH), 0.6 (3H, s, CH₃), 1.0 (3H, s, CH₃), 1.9 (3H, s, CH₃), 2.0 (3H, s, CH₃), 2.4 (3H, s, CH₃), 3.3 (3H, s, CH₃); *fac*-**5** δ =−31.8 (3H, s, CH), −6.4 (9H, s, CH₃CO), −5.3 (3H, s, CH₃CH₂), −3.3 (3H, s, CH₃CH₂), 2.6 (9H, s, CH₃CH₂) (these were obtained from an isomeric mixture by subtracting the peaks of *mer*-**5**); *mer*-**5** δ =−41.7 (1H, s, CH), −31.5 (1H, s, CH), −22.0 (1H, s, CH), −11.4 (3H, s, CH₃CO), −10.0 (1H, s, CH₃CH₂), −7.9 (1H, s, CH₃CH₂), −5.6 (3H, s, CH₃CO), −5.0 (1H, s, CH₃CH₂), −3.7 (1H, s, CH₃CH₂), −1.1 (3H, s, CH₃CO), −0.3 (1H, s, CH₃CH₂), 0.7 (1H, s, CH₃CH₂), 2.3 (3H, s, CH₃CH₂), 2.5 (3H, s, CH₃CH₂), 2.6 (3H, s, CH₃CH₂). Half-wave potentials for one-electron steps in 0.1 mol dm^{−3} (C₂H₅)₄NClO₄-acetonitrile vs. Ag|0.1 mol dm^{−3} AgClO₄-

acetonitrile at 25 °C: *mer*-**2**, −0.48 V (Nernstian reduction) and 1.29 V (quasi-reversible oxidation); *mer*-**3**, −0.50 V (Nernstian reduction) and 1.28 V (quasi-reversible oxidation).

Other Chemicals. *N,N*-Dimethylformamide (DMF) was spectral reagent grade (Dojindo Laboratories, Dotite Spectrosol). Acetonitrile (AN) was purified as described previously.¹³ Benzene and hexane used in chromatography were chromatographic grade solvents (Wako Pure Chemical Industries, Ltd.), and the other chemicals were of reagent grade.

Apparatus. A Shimadzu Seisakusho Ltd. CHN Analyzer CHN-1A was used for the elemental analyses. UV-vis spectra were measured with a Hitachi Model 200-20 spectrophotometer, and ¹H NMR spectra with a JEOL JMN GX270. The light sources for photochemical experiments were a 32 W low-pressure mercury lamp (Riko Kagaku Sangyo, UVL-321LA) and a 250 W high-pressure mercury lamp (Ushio Model UI-501C). High-performance liquid chromatography (HPLC) was carried out by means of a Toyo Soda apparatus consisting of a CCPM solvent delivery system, a UV-8000 spectrophotometric monitor, and a TSK gel ODS-80T_m column (4.6 mm i.d.×150 mm, Toyo Soda).

Measurement of Isomerization Rates. A weighed sample (about 0.025 mmol) of each isolated isomer of **1**–**4** was dissolved in 25 cm³ of DMF. The solution was transferred into a 30 cm³ flask containing a magnetic stirrer bar. The flask was immersed in an oil bath (thermostated within ± 1 °C) placed on a magnetic stirrer, which was at once put in motion. Small aliquots (ca. 5 mm³ each) were taken out of the solution at suitable time intervals by means of a microsyringe which had been kept at room temperature, and 4 mm³ of the aliquot was immediately injected into the HPLC system.

The compositions of the mobile phases used are given in Table 2 together with the retention times. The flow rate was 1 cm³ min^{−1}. The spectrophotometric monitor was operated at the wave length of the π - π^* absorption band^{14,15} of each pair of the isomers (Table 2).

The product of the HPLC peak height and the half-peak width was proportional to the amount of the isomer injected. The isomeric concentrations in each aliquot were determined by means of the calibration curves that had been drawn for standard series of mixtures prepared gravimetrically from the isolated samples of the isomers. Statistical tests showed that the main source of error of the HPLC determination was the day-to-day variance. The reproducibility was estimated to be within 4%.

The isomerization of **4** in AN solutions was carried out in a similar way. The mixture was refluxed on an oil bath kept at 90 °C. The reaction temperature was practically the

Table 2. Compositions of the Mobile Phases for HPLC, the Operating Wavelengths (λ), and the Retention Times (t_r) of the Isomers

Complex	Solvent (volume fraction)	λ nm	t_r /min	
			<i>fac</i>	<i>mer</i>
1	AN(0.7)-H ₂ O	275	6.8	7.2
2	AN(0.075)-H ₂ O(0.225)-MeOH	276	8.7	9.2
3	AN(0.9)-H ₂ O	277	5.0	4.7
4	AN(0.95)-H ₂ O	277	5.1	4.5

normal boiling point of the solvent (81.6 °C).

Molecular Orbital Calculation. The calculation was based on a modified variety of the extended Hückel method. Computation was carried out on an NEC ACOS-850 at the Computer Center of Sophia University for the facial isomers of **1–5** and two representative meridional isomers (**1** and **4**). The details of the procedure and the results are described elsewhere,¹⁵⁾ and only the atomic bond populations for the Ru–O bonds are presented here.

Results

Qualitative Observations. Isomerization of **1 in Various Solvents:** The meridional isomer was dissolved in a deoxygenated solvent to ca. 1 mol m⁻³. The solution was refluxed for ca. 20 h under an argon atmosphere on an oil bath kept at a temperature 5 °C higher than the normal boiling point of the solvent; it was then examined for the presence of the facial isomer by means of thin-layer chromatography on Merck Kieselgel 60 (developing solvent, hexane–benzene, 5 : 8 by volume).

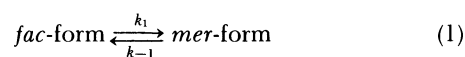
The results are presented in Table 3. In the first four solvents, neither the facial isomer nor any other product was detected even when the refluxing was prolonged to more than 30 h. In pyridine, the color changed from red to dark green only by allowing the solution to stand overnight at room temperature, indicating that decomposition and/or ligand exchange took place; no facial isomer was detected in the resultant solution. In the other ten solvents, the isomerization occurred more or less rapidly, and the facial isomer was accompanied by some amounts of one or more by-products, which appeared to be ruthenium species produced by partial ligand exchange.

The isomerization of *mer-1* did not occur photo-

chemically. Irradiation of its AN solutions under an argon atmosphere with the high-pressure mercury lamp for 9.5 h or with the low-pressure mercury lamp for 25.5 h at room temperatures yielded a small amount of a decomposition product, but no facial isomer was detected. The irradiation of *mer-1* in ethanol with the low-pressure mercury lamp did not bring about the isomerization either; instead, *mer-1* was reduced to the corresponding ruthenium(II) species, which was completely reoxidized back to the original meridional isomer by atmospheric oxygen. This result agrees with the observation reported by Gordon et al.⁴⁾ that no isomerization accompanied the chemical reduction and reoxidation.

Isomerization in DMF: The results are indicated in Table 1. Complexes **5** and **6** did not undergo any isomerization in DMF even after being refluxed (ca. 158 °C) for more than 30 h, while **7**, **8**, and **9** were reduced to the corresponding ruthenium(II) species. Complexes **1**, **2**, **3**, and **4** underwent the isomerization when heated in DMF, and their kinetics were studied quantitatively.

Determination of the Rate Constants and Equilibrium Constants. A typical set of isomeric concentration–time curves is shown in Fig. 2. Since preliminary experiments showed that the half-lives of the facial-to-meridional isomerization and its backward reaction



were independent of the initial concentration, they were treated as essentially reversible, first-order reactions. But the isomerization reactions were accompanied by slow decomposition, as is seen from Fig. 2.

It can be readily shown that Eq. 2 holds if the decomposition is irreversible and follows the first-order rate law with respect to the total concentration of the facial and the meridional isomers:

$$-\ln\{(x - x_e)/(x_0 - x_e)\} = (k_1 + k_{-1})t. \quad (2)$$

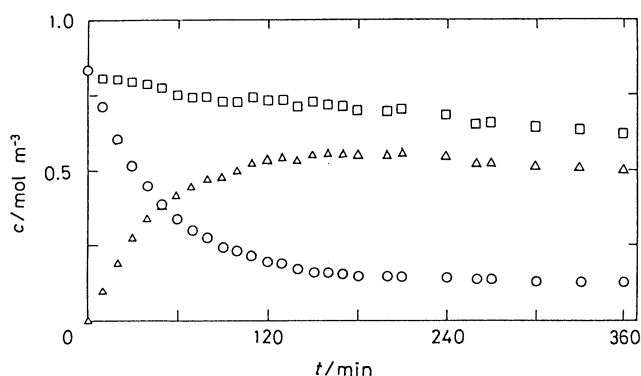


Fig. 2. Concentration–time curves for the reaction of *fac-1* in DMF at 90 °C.
○, [*fac-1*]; △, [*mer-1*]; □, [*fac-1*] + [*mer-1*].

Table 3. Some Physical Properties^{a)} of the Solvents and the Isomerization of *mer-1* Therein

Solvent	<i>t</i> _b /°C ^{b)}	ε _r ^{c)}	μ/μ _D ^{d)}	<i>fac-1</i> ^{e)}
Benzene	80.1	2.27	0	—
Toluene	110.6	2.38	0.31	—
Chloroform	61.2	4.81	1.15	—
Chlorobenzene	131.7	5.62	1.62	—
1,1,2,2-Tetrachlorobenzene	145.1	8.20*	1.71	+
Trifluoroacetic acid	71.8	8.55*	2.28	+
Pyridine	115.3	12.9	2.37	f)
1-Butanol	117.7	17.5	1.75	+
2-Propanol	82.2	19.9	1.66	+
1-Propanol	97.2	20.5	3.09	+
Ethanol	78.3	24.6	1.66	+
Methanol	64.5	32.7	2.87	+
<i>N,N</i> -Dimethylformamide	153.0	36.7	3.24	+
Acetonitrile	81.6	35.9	3.53	+
1,1,1-Trifluoroethanol	74.1	—	—	+

a) From Ref. 19. b) Normal boiling temperature. c) Relative permittivity at 25 °C or at 20 °C (those marked by asterisks). d) Dipole moment; μ_D = 3.336 × 10⁻³⁰ C m. e) +, detected accompanied by by-product(s) after ca. 20 h of refluxing; —, not detected. f) Decomposition and/or ligand exchange.

Here x is the isomeric fraction of the facial isomer at time t as defined by Eq. 3

$$x = [\text{fac}] / ([\text{fac}] + [\text{mer}]), \quad (3)$$

where the brackets mean the amount-of-substance concentration at time t of the specified isomer; x_e is its equilibrium value, and x_0 is the initial value of x .

In the present cases, the rates of decomposition were actually proportional to the total concentration of the two isomers with rate constants less than ca. 7% of $k_1 + k_{-1}$.

The present experimental procedure inevitably involved a time lag; it took some time for the temperature of the reaction mixture, T , to reach the bath temperature, T_b . The reaction gradually accelerated during this time lag, and the plot of the left-hand side of Eq. 2 against t became distorted at small times. But beyond a short period (ca. 6 min in the most unfavorable cases), the plot became linear. The values of $k_1 + k_{-1}$ were obtained from the slope of the linear portion.

A separate experiment showed that the variation of T followed the Newton's law of heat flow, that is, $dT/dt = a(T_b - T)$ with $a = 8.85 \times 10^{-3} \text{ s}^{-1}$ for the present experimental arrangement. Digital simulations were carried out on the basis of this value of a and the actual activation energies. Their results reproduced the experimental plots quite well and ascertained that the slope of the linear portion gave exactly the value of $k_1 + k_{-1}$.

The equilibrium constant of reaction (1) is defined by

$$K = [\text{mer}]_e / [\text{fac}]_e = k_1 / k_{-1} = (1 - x_e) / x_e. \quad (4)$$

Their values were obtained in the following way, instead of direct measurement of the equilibrium concentrations, in order to avoid possible errors owing to extensive decomposition brought about by prolonged heating and to increase the precision by making use of as many data points as feasible.

Two parallel kinetic runs were carried out: one (run a) was started with a solution of pure facial isomer ($x_0 = 1$), and the other (run b) with a solution of pure meridional isomer ($x_0 = 0$). In run a, the fraction of the meridional form at time t_a , $1 - x_a$, was determined; in run b, the fraction of the facial form at time t_b , x_b , was determined. Equation 1 shows that

$$1 - x_a = (1 - x_e) [1 - \exp\{-(k_1 + k_{-1})t_a\}]$$

and

$$x_b = x_e [1 - \exp\{-(k_1 + k_{-1})t_b\}],$$

so that

$$(1 - x_a) / x_b = \{ (1 - x_e) / x_e \} = fK, \quad (5)$$

where

$$f = [1 - \exp\{-(k_1 + k_{-1})t_a\}] / [1 - \exp\{-(k_1 + k_{-1})t_b\}].$$

The left-hand side of Eq. 5 would give the K value if t_a could be made exactly equal to t_b . In practice, there

was some uncertainty in both t_a and t_b owing to the above-mentioned time lag, and the experimental values of $(1 - x_a) / x_b$ at shorter times showed deviating fluctuations. Only the points that gave stable values were used for calculating the mean values of K . The f values of these points were between 0.99 and 1.01 for $t_a - t_b$ up to ± 6 min, the largest time lag ever observed.

The equilibrium constants obtained in this way are listed in Table 4. No definite temperature dependence was detectable except for **3**. In the case of **3**, the plot of $\ln K$ against T^{-1} was fairly linear, and its linear regression line had a slope which was statistically non-zero at 10% significance level. The slope would give the standard reaction enthalpy value of $(3.4 \pm 3.2) \text{ kJ mol}^{-1}$. This non-zero slope, however, is very likely to be accidental, in view of the fact that the determinations of the equilibrium constants of this complex (and **2**, too) were difficult owing to relatively poor separation between the chromatographic peaks and the larger extent of the decomposition. It was, therefore, decided that the equilibrium constant was independent of the temperature, and the values for the four temperatures were averaged. In the case of **2**, the value for 373 K was excluded from the average, because its deviation was almost statistically significant at 5% significance level.

The left-hand side of Eq. 2 was calculated with the

Table 4. Equilibrium Constants (K) of Facial-to-Meridional Isomerization Reactions in DMF and Their Forward (k_1) and Backward (k_{-1}) Rate Constants

Complex	T/K	K^a	$k_1 + k_{-1}$	k_1	k_{-1}
			10^{-5} s^{-1}	10^{-5} s^{-1}	10^{-5} s^{-1}
1	343	4.24	4.83	3.91	0.917
	353	4.32	12.4	10.0	2.35
	363	4.20	32.8	26.6	6.22
	373	4.30	77.2	62.6	14.6
	average	4.27 \pm 0.13			
2	343	2.76	6.04	4.41	1.62
	353	2.64	16.1	11.8	4.33
	363	2.75	35.6	26.0	9.57
	(373)	(2.39) ^b	72.4	52.9	19.5
	average	2.72 \pm 0.19			
3	343	2.50	15.4	11.2	4.21
	353	2.68	25.5	18.5	6.97
	363	2.65	51.9	37.7	14.2
	373	2.79	107	77.8	29.2
	average	2.66 \pm 0.28			
4	343	1.71	15.3	9.69	5.57
	353	1.74	32.1	20.4	11.7
	363	1.80	74.0	47.0	27.0
	373	1.71	160	102	58.6
	average	1.74 \pm 0.10			

a) The uncertainties are 90% confidence limits. b) Not included in the average.

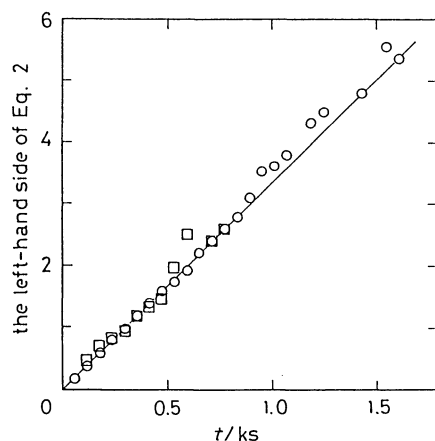


Fig. 3. The left-hand side of Eq. 2 plotted against the reaction time, t , for the reactions of **1** in DMF at 90°C.

Starting isomer: ○, *fac*-**1**; □, *mer*-**1**.

value of x_e obtained from the K value and plotted against t . The plots were quite linear until the magnitude of the logarithmic term reached ca. 2.5–3 except for the deviations due to the time lag, which were noticeable during the initial period of a few runs with higher bath temperatures. An example is given in Fig. 3 (here the effect of the time lag is barely perceptible). The slopes of the plots were independent of the isomeric form with which the reactions were started. The individual values of k_1 and k_{-1} listed in Table 4 were calculated from the slope and the K value.

Kinetic Parameters. If the equilibrium constant is independent of the temperature, the standard enthalpies of activation of the forward and the backward reactions are the same (ΔH^\ddagger). The ΔH^\ddagger value and the standard entropies of activation of the forward and backward reactions (ΔS_1^\ddagger and ΔS_{-1}^\ddagger , respectively) were obtained on the basis of the following equations, by plotting the logarithmic value of $(k_1 + k_{-1})/T$ against $1/T$:

$$\ln\{(k_1 + k_{-1})/T\}/s^{-1} K^{-1} = -\Delta H^\ddagger/RT + A'$$

$$\Delta S_1^\ddagger/R = A' - \ln(k_B h^{-1}/s^{-1} K^{-1}) - \ln(1 + K^{-1})$$

$$\Delta S_{-1}^\ddagger/R = A' - \ln(k_B h^{-1}/s^{-1} K^{-1}) + \ln(1 + K)$$

Here k_B is the Boltzmann constant and h is the Planck

Table 5. Standard Enthalpies (ΔH^\ddagger) and Entropies (ΔS^\ddagger) of Activation^{a)}

Comoplex	$\Delta H^\ddagger/\text{kJ mol}^{-1}$	$-\Delta S_1^\ddagger/R^b)$	$-\Delta S_{-1}^\ddagger/R^b)$
1	96.0 ± 3.3	6.1	7.6 ± 1.1
2	85.0 ± 9.5	9.8	10.8 ± 3.2
3	66.4 ± 14.6	15.5	16.5 ± 4.9
4	81.1 ± 3.0	10.4	11.0 ± 1.0

a) The uncertainties are 90% confidence limits. b) R is the gas constant, ca. $8.314 \text{ J mol}^{-1} \text{ K}^{-1}$. Subscripts 1 and -1 refer to *fac*-to-*mer* and *mer*-to-*fac* reactions, respectively. The uncertainties apply to both ΔS^\ddagger values.

Table 6. Effect of Electrolytes on $(k_1 + k_{-1})/10^{-5} \text{ s}^{-1}$ of the Isomerization of *fac*-**4** in Acetonitrile, at ca. 82°C

Electrolyte	Concentration/mol dm ⁻³			
	0.10	0.02	0.01	0
$\text{N}(\text{C}_2\text{H}_5)_4\text{ClO}_4$	2.86	2.80	2.78	2.19 ^{a)}
$\text{Mg}(\text{ClO}_4)_2$	2.67	2.66	2.68	
CH_3COOH	3.11	2.92	2.80	

a) The equilibrium constant was 1.83.

constant.

The plots were fairly linear. The point for 343 K in the case of **3** appeared to deviate more than the other points did, but the deviation was not statistically significant enough to exclude the point as an outlying one. The values of the kinetic parameters are presented in Table 5.

Effects of Electrolytes. Effects of some electrolytes on the rate of the isomerization of *fac*-**4** were examined by refluxing it in AN instead of DMF, since solubilities of the electrolytes in the latter solvent were insufficient. The reaction temperature was ca. 82°C. The values of $k_1 + k_{-1}$ are listed in Table 6.

Discussion

Effects of Solvents and Electrolytes. The kind of solvent largely influenced the rate of isomerization of *mer*-**1** (Table 3). The isomerization was observed in solvents with higher relative permittivities, except for pyridine, in which the complex was decomposed.

Solvent-assisted bond-rupture mechanisms (e.g., Ref. 2) is compatible with this fact and with the observation that the resultant *fac*-**1** was always accompanied by by-products. An intermediate with a dangling ligand is formed when an Ru-O bond is attacked by solvent molecules. The open end of the dangling ligand may recombine with the central atom either at the original position or at some other position, the latter case leading to the isomerization. The solvent must be a coordinating agent powerful enough to break the Ru-O bond. But it should not be so too much; then the dangling end fails to recombine, and ligand exchange or decomposition predominates, as was the case of the reaction in pyridine, a strong coordinative agent.

The isomerization rate of **1** in AN was not affected by the addition of the free ligand, 1,1,1-trifluoro-2,4-pentanedione, up to 1 mol dm^{-3} ; but its addition appeared to reduce the extent of the decomposition. This observation will indicate that the isomerization is a solvent-assisted intramolecular process and the decomposition is ligand-exchange by solvent.

The addition of tetraethylammonium perchlorate and magnesium perchlorate increased the isomerization rate of *fac*-**4** in AN; the addition of acetic acid produced an even larger increase (Table 6). The presence of ions may assist the bond rupture through

the relaxation of the charge separation accompanying the bond rupture. But there seem to be contributions of more specific interaction, since acetic acid is a very weak electrolyte in AN.¹⁶⁾ Their quantitative interpretation is difficult at this stage.

Effects of Substituents. Trifluoromethyl Group:

All the complexes for which the facial-meridional isomerization was observed in DMF have trifluoromethyl groups (Table 3). To the authors' knowledge, the ruthenium(III) complexes that so far have been reported to undergo isomeric rearrangement are fluorine substituted β -diketonato complexes, with one exception of tris[(+)-3-acetylcamphorato]ruthenium(III).¹⁷⁾ Fay et al.⁵⁾ reported that no conversion of the optical isomers of tris(acetylacetonato)ruthenium(III) was observed when they were heated in chlorobenzene for 10 h at 165 °C. Complexes **7**, **8**, and **9** would isomerize, were they not reduced when heated in DMF. There is an indication that the equilibrium constants for these three complexes will be almost the same and quite large (see the next subsection). The fact that the facial form of **7** could not be obtained is attributable to experimental difficulty rather than to the absence of isomerization.

The presence of trifluoromethyl group, therefore, appears to be a necessary condition for a β -diketonato ruthenium(III) complex to undergo the facial-meridional isomerization with appreciable rates. The primary reason is that a trifluoromethyl group, being strongly electron-withdrawing, "weakens and lengthens metal-oxygen bonds, thereby facilitating rearrangement."⁴⁾ This view is substantiated by a molecular orbital calculation, as will be discussed later.

Equilibrium Constants: Gordon et al.⁴⁾ reported that the equilibrium constant of reaction (1) for **1** in 1,1,2,2-tetrachloroethane at 150 °C was 4.9 with $\Delta_r H^\circ = (-4.6 \pm 2.5)$ kJ mol⁻¹ and $\Delta_r S^\circ = (+2.5 \pm 5.9)$ J mol⁻¹ K⁻¹. This equilibrium constant is quite close to the present result in DMF at 70–100 °C (Table 4). On the other hand, $\Delta_r H^\circ$ was not detectable in our case. In view of the present experimental errors, a value of $|\Delta_r H^\circ|$ amounting to 2.5 kJ mol⁻¹ or more should have been detected.

This discrepancy may be explained in terms of the relative permittivities of the two solvents (Table 3). In each solvent, the major part of the standard affinity of the isomerization will probably be the difference between the solvation Gibbs energies of the facial and the meridional isomers, and these solvation energies will arise mainly from the electrostatic interaction between the polar isomer molecules and the dielectric solvent. By analogy to the ion-dielectric interaction, it is likely that the standard enthalpy of such an interaction will be proportional to $\epsilon_r^{-1} - T(d\epsilon_r^{-1}/dT)$. For various common solvents near room temperature, ϵ_r follows the empirical formula $\epsilon_r = \epsilon_r^\circ \exp(-T/\theta)$, where the characteristic temperature θ usually lies

quite near the normal melting point of the solvent (T_{fus}).¹⁸⁾ Then, $\Delta_r H^\circ$ will be roughly proportional to the factor $(1 - T/T_{\text{fus}})/\epsilon_r$. The value of this factor is -0.18 for the tetrachloroethane ($T_{\text{fus}} = 229.3$ K¹⁹⁾) at 150 °C, and it is -0.03 for DMF ($T_{\text{fus}} = 212.7$ K¹⁹⁾) at 100 °C.

The K values (Table 4) are not very much different from 3, the value expected if the equilibrium is determined solely by the probability. But they show a tendency: K decreases with the increase in the electron donating character of the substituent R'. A fairly straight line is obtained when $\ln K$ is plotted against the reversible half-wave potential of the Ru^{III}/Ru^{II} process of the complex (Fig. 4) or against the Hammett constant of R' (a linear relationship has been established between the reversible half-wave potential and the sum of the Hammett constants of the substituents¹³⁾). This linearity, being based on only four points, cannot be generalized too much. But if its extrapolation is allowed, the K values for complex **7**, **8**, and **9**, whose half-wave potentials were -0.33 V, -0.32 V, and -0.33 V, respectively,¹³⁾ will be around 16.

It is difficult to explain this tendency quantitatively. The following is one possibility. Quite likely the entropy of solvation plays a decisive role, since the standard reaction Gibbs energies were essentially entropic. There will be two opposite factors. One is the decrease of entropy caused by the orientation of solvent molecules around the dipolar complex species. This decrease makes the facial form less favorable in terms of entropy, because it always has a larger dipole moment than that of the corresponding meridional form. This effect will play an important role in mildly polar and less structured solvents. The other factor, however, comes into effect in a highly

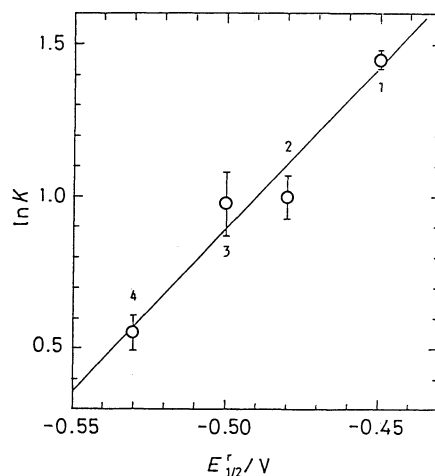


Fig. 4. Correlation between $\ln K$ and the reversible half-wave potential of the Ru^{III}/Ru^{II} process in 0.1 mol dm⁻³ (C₂H₅)₄NClO₄ in AN at 25 °C vs. Ag|0.1 mol dm⁻³ AgClO₄-AN ($E'_{1/2}$). The error bars represent 90% confidence limits; correlation coefficient=0.9756.

associated or structured solvent like DMF (its entropy of evaporation is $90.0 \text{ J mol}^{-1} \text{ K}^{-1}$ ¹⁹⁾). Then the structure of the solvent will be broken by the presence of strongly dipolar solute molecules and an increase of entropy results, thereby making the facial form more favorable. Even in DMF, the first factor seems to predominate in the case of **1**. But as the substituent R' becomes more and more strongly electron-donating and bulky, the second factor will overcome the first, and the K value becomes progressively smaller than 3.

Whatever the reason may be, there is an interesting parallelism in the HPLC retention times. With AN-water mixtures of various compositions, the retention time (t_r) of each complex increased with the water content. In a given mixture, the t_r value of *fac*-**1** was smaller than that of *mer*-**1**, indicating that the *fac*-form was more stable in a polar mobile phase. In the cases of **3** and **4**, on the contrary, the order was reversed (Table 2); the *fac*-forms are less stable, in spite of their higher polarity.

Enthalpies of Activation: For the isomerization of **1** in 1,1,2,2-tetrachloroethane at $140.5\text{--}174.5^\circ\text{C}$,⁴⁾ $\Delta H^\ddagger/\text{kJ mol}^{-1}$ is 138 ± 3.3 (*fac*-to-*mer*) and 118 ± 4.6 (*mer*-to-*fac*). These are a little larger than the present value (Table 5), probably reflecting the smaller dielectric character of the chloroethane. The entropy of activation for the *fac*-to-*mer* reaction, $\Delta S_1^\ddagger/R = -3.8 \pm 1.0$, is larger and that for the reverse reaction, $\Delta S_{-1}^\ddagger/R = -11.5 \pm 1.5$, is smaller than the corresponding present values.

The enthalpy of activation, showing a minimum at complex **3**, cannot be simply related to the half-wave potential or the Hammett constant, since the latter vary monotonically. But it will be related to the robustness of the Ru-O bonds, if the isomerization proceeds via a solvent-assisted bond-rupture mechanism. One of the measures of bond strength is the atomic bond population,²⁰⁾ which is believed to be proportional to the bond order. The values obtained by means of a modified extended Hückel method are presented in Table 7. Results of such a calculation

Table 7. Atomic Bond Populations of Ru-O Bonds Calculated by Means of the Modified Extended Hückel MO Method¹⁵⁾

Ru-O bond ^{a)}	Complex				
	1	2	3	4	5
<i>fac</i>					
a, c, d	0.244	0.240	0.240	0.241	0.251
b, e, f	0.237	0.234	0.233	0.235	0.250
<i>mer</i>					
a'	0.242			0.239	
b'	0.238			0.236	
c'	0.240			0.238	
d'	0.244			0.241	
e'	0.239			0.238	
f'	0.242			0.238	

a) For the bond designation, see Fig. 1.

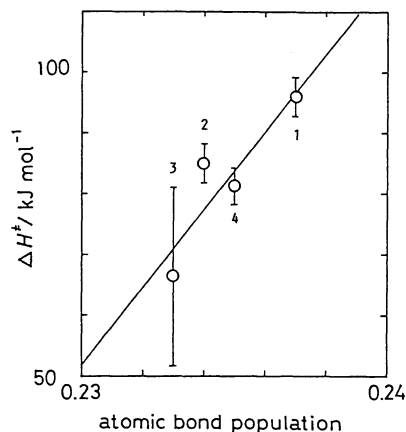


Fig. 5. Correlation between ΔH^\ddagger and the atomic bond population of the Ru-O bonds b, e, and f. The error bars represent 90% confidence limits; correlation coefficient = 0.8985.

are generally not precise. Nevertheless, in these particular instances, where all the compounds are very similar, the values of atomic bond population will correctly reflect the relative robustness of the bond.

The facial isomer has two distinguishable kinds of Ru-O bonds: the atomic bond population of the three Ru-O bonds that are adjacent to the substituents R' (bonds b, e, and f in Fig. 1) is lower than that of the others in each complex. There is a fairly linear correlation between ΔH^\ddagger and the atomic bond population of the former Ru-O bonds, as shown in Fig. 5. This may indicate that the isomerization is initiated by the rupture of the least robust Ru-O bond.

The bond rupture mechanisms can be classified according to the idealized geometry of the transition state: trigonal bipyramidal (TBP) or square pyramidal (SP). The rupture of the bonds a', c', e', or f' is required for the *mer*-to-*fac* conversion to occur through the TBP transition states, whereas the rupture of any bond leads to the *fac*-to-*mer* conversion through both transition states.²⁾ It is tempting to suggest that the isomerization involved the SP transition states, in view of the result that the least robust bond in the meridional form was the bond b'. Drawing such an inference, however, will be too early because the reaction may involve more than one type of transition state.²⁾

The calculated values clearly indicate the weakening effect of trifluoromethyl group.⁴⁾ The atomic bond population of *fac*-**5**, 0.250, is very much higher than those of the trifluoromethyl-substituted complexes. If the above linear correlation is extrapolated to this value, ΔH^\ddagger of **5** will be ca. 180 kJ mol^{-1} . With such a large value of ΔH^\ddagger , $k_1 + k_{-1}$ at 100°C would be of the order of 10^{-15} s^{-1} or less.

The authors are very grateful to Prof. Hiroshi Kobayashi of Kitazato University not only for many valuable suggestions and encouraging discussions,

but also his kindness in providing them with the program of the original Hückel method. They also thank Dr. S. F. Howell, Sophia University, for correcting the manuscript. The elemental analyses were carried out by Mrs. Nakako Tokita and the NMR measurement by Mrs. Hiroko Kin and Mrs. Yukari Suetsugu of the Department of Chemistry, to whom the authors' thanks are due.

References

- 1) R. C. Fay and T. S. Piper, *Inorg. Chem.*, **3**, 348 (1964).
- 2) J. G. Gordon, II, and R. H. Holm, *J. Am. Chem. Soc.*, **92**, 5319 (1970).
- 3) A. Y. Girgis and R. C. Fay, *J. Am. Chem. Soc.*, **92**, 7061 (1970).
- 4) J. G. Gordon, II, M. J. O'Connor, and R. H. Holm, *Inorg. Chim. Acta*, **5**, 381 (1971).
- 5) R. C. Fay, A. Y. Girgis, and U. Klabunde, *J. Am. Chem. Soc.*, **92**, 7056 (1970).
- 6) J. R. Hutchinson, J. G. Gordon, II, and R. H. Holm, *Inorg. Chem.*, **10**, 1004 (1971).
- 7) C. Kutal and R. E. Sievers, *Inorg. Chem.*, **13**, 897 (1974).
- 8) K. Saito, *Pure Appl. Chem.*, **38**, 325 (1974).
- 9) Y. Hoshino, R. Takahashi, K. Shimizu, G. P. Satô, and K. Aoki, *Bull. Chem. Soc. Jpn.*, **62**, 993 (1989).
- 10) A. Endo, K. Shimizu, G. P. Satô, and M. Mukaida, *Chem. Lett.*, **1984**, 437; A. Endo, M. Kajitani, M. Mukaida, K. Shimizu, and G. P. Satô, *Inorg. Chim. Acta*, **150**, 25 (1988).
- 11) J. C. Reid and M. Calvin, *J. Am. Chem. Soc.*, **72**, 325 (1950).
- 12) Y. Hoshino, Y. Yukawa, A. Endo, K. Shimizu, and G. P. Satô, *Chem. Lett.*, **1987**, 845.
- 13) A. Endo, Y. Hoshino, K. Hirakata, Y. Takeuchi, K. Shimizu, Y. Furushima, H. Ikeuchi, and G. P. Satô, *Bull. Chem. Soc. Jpn.*, **62**, 709 (1989).
- 14) H. Kobayashi, H. Matsuzawa, Y. Kaizu, and A. Ichida, *Inorg. Chem.*, **26**, 4318 (1987).
- 15) Y. Satsu, Ph. D. Thesis, Sophia University, Tokyo, 1987.
- 16) The Chemical Society of Japan, "Kagaku Binran," Maruzen, Tokyo (1984), p.II-343.
- 17) G. W. Everett, Jr. and R. H. Holm, *J. Am. Chem. Soc.*, **96**, 2087 (1974).
- 18) R. W. Gurney, "Ionic Processes in Solution," McGraw-Hill, New York, Toronto, London (1953), Chap. 1.
- 19) J. A. Riddick, W. B. Bunger, and T. K. Sakano, "Organic Solvents, Physical Properties and Methods of Purification," in "Techniques of Chemistry," 4th ed, ed by A. Weissberger, John Wiley & Sons, New York, Chichester, Brisbane, Toronto, Singapore (1986), Vol. II.
- 20) R. S. Mulliken, *J. Chem. Phys.*, **23**, 1841 (1955).